Are low-energy nuclear observables sensitive to high-energy phase shifts?

S.K. Bogner[1], R.J. Furnstahl[1], R.J. Perry[1], A. Schwenk[2]

[1] *Department of Physics, The Ohio State University, Columbus, OH 43210*
[2] *TRIUMF, 4004 Wesbrook Mall, Vancouver, BC, Canada, V6T 2A3*

Abstract

Conventional nucleon-nucleon potentials with strong short-range repulsion require contributions from high-momentum wave function components even for low-energy observables such as the deuteron binding energy. This can lead to the misconception that reproducing high-energy phase shifts is important for such observables. Interactions derived via the similarity renormalization group decouple high-energy and low-energy physics while preserving the phase shifts from the starting potential. They are used to show that high-momentum components (and high-energy phase shifts) can be set to zero when using low-momentum interactions, without losing information relevant for low-energy observables.

1 Introduction

High-momentum degrees of freedom do not automatically decouple from low-energy observables, especially for conventional nucleon-nucleon (NN) potentials. For instance, nuclear forces are typically fit to scattering data up to where inelasticities start to become significant, $E_{\rm lab} \sim 350\,\mathrm{MeV}$ or relative momenta $k \sim 2\,\mathrm{fm}^{-1}$. However, most NN potentials have significant high-momentum ($k > 2\,\mathrm{fm}^{-1}$) off-diagonal matrix elements that require summations over high-energy intermediate states, even if one is calculating low-energy observables. If such interactions are simply truncated at $2\,\mathrm{fm}^{-1}$, the deuteron binding energy along with S-wave phase shifts down to zero energy are drastically altered.

Email addresses:
bogner@mps.ohio-state.edu (S.K. Bogner),
furnstahl.1@osu.edu (R.J. Furnstahl),
perry@mps.ohio-state.edu (R.J. Perry),
schwenk@triumf.ca (A. Schwenk).

This can lead to the misconception that *details* of strong-interaction dynamics above some energy scale are relevant to low-energy nuclear structure and reactions. Such a brute-force cutoff, however, does not disentangle high-energy (short-distance) features from low-energy (long-distance) observables. To do so, it is necessary to integrate out (and thus separate) irrelevant short-distance details from their effects on low-energy observables. This is achieved by the renormalization group.

Renormalization group (RG) transformations that lower a cutoff in relative momentum have been used to derive NN potentials that have vanishing matrix elements for momenta above the cutoff. Such interactions, known generically as $V_{\mathrm{low}\,k}$, show greatly enhanced convergence properties in nuclear few- and many-body systems for cutoffs of order $\Lambda = 2\,\mathrm{fm}^{-1}$ or lower [1,2,3,4,5,6,7]. However, the initial NN potentials (typically cut off at 4–5 fm^{-1}) predict nonzero elastic phase shifts to much higher energies than $E_{\mathrm{lab}} \sim 350\,\mathrm{MeV}$, which in some channels are semi-quantitatively consistent with experiment. In contrast, phase shifts from $V_{\mathrm{low}\,k}$ as usually implemented are zero above the cutoff. This discrepancy has led to some uneasiness that important information may be lost with $V_{\mathrm{low}\,k}$. Similar concerns have been expressed about effective field theory (EFT) potentials.

This unease is exacerbated by experience with conventional NN potentials, which feature strong short-range repulsion. The repulsion causes even bound states with very low energies (such as the deuteron) to have important contributions to the binding and other properties from high-momentum components (well above $2\,\mathrm{fm}^{-1}$) of the deuteron wave function. In Ref. [8], the authors calculate cross sections for electron scattering from the deuteron using as input a spectral function that is the momentum distribution times a delta function in energy. After noting the effect of excluding high momenta on the cross section, they conclude: "and thus the data confirm the existence of high-momentum components in the deuteron wave function" [8]. These observations reinforce the intuition that there is information in quantitatively reproducing high-energy phase shifts that is lost when evolving to low-momentum interactions. In this paper, we use the similarity renormalization group (SRG) [9,10,11,12] as a tool to demonstrate unequivocally that this intuition is incorrect.

A fundamental tenet of renormalization theory is that the *relevant* details of high-energy physics for calculating low-energy observables can be captured in the scale-dependent coefficients of operators in a low-energy hamiltonian [13]. This principle does not mean that high-energy and low-energy physics is entirely decoupled in an effective theory. In fact, it implies that we can include as much irrelevant coupling to *incorrect* high-energy physics as we want by using a large cutoff, with no consequence to low-energy predictions (assuming we can calculate accurately). But this freedom also offers the possibility of decoupling, which makes practical calculations more tractable by restricting

the necessary degrees of freedom. This decoupling can be efficiently achieved by evolving nuclear interactions using RG transformations.

The SRG allows for particularly transparent and convincing demonstrations of decoupling, because the evolution of the hamiltonian and other operators proceeds via transformations that can be chosen to be unitary, so that all observables are explicitly preserved. Thus, when we include the full set of momentum states used for the original potential with the evolved potential V_s, we find the same deuteron binding energy and phase shifts for all energies. However, the evolved V_s explicitly decouples high-energy dynamics from low-energy observables, which means that we can exclude the high-momentum parts (so that we have a low-momentum potential like $V_{\mathrm{low}\,k}$) without disturbing the information content (phase shifts and deuteron binding energy) at lower energies. We apply a similar test to the SRG-evolved deuteron momentum distribution to show that high-momentum effects in low-energy bound states are captured by scale-dependent low-momentum operators.

2 Background on the SRG

In Ref. [12], the similarity renormalization group (SRG) approach is applied to NN interactions. The SRG was developed by Glazek and Wilson [9], while Wegner [10] independently developed a related but simpler set of flow equations. The formalism we employ closely resembles that of Wegner, but we find that a transformation even simpler than advocated by Wegner is robust and adequate for all calculations to date.

The evolution or flow of the hamiltonian with a parameter s follows from a unitary transformation,

$$H_s = U(s) H U^\dagger(s) \equiv T_{\mathrm{rel}} + V_s \,, \tag{1}$$

where T_{rel} is the relative kinetic energy and $H = T_{\mathrm{rel}} + V$ is the initial hamiltonian in the center-of-mass system. Eq. (1) defines the evolved potential V_s, with T_{rel} taken to be independent of s. Then H_s evolves according to

$$\frac{dH_s}{ds} = [\eta(s), H_s] \,, \tag{2}$$

with

$$\eta(s) = \frac{dU(s)}{ds} U^\dagger(s) = -\eta^\dagger(s) \,. \tag{3}$$

Choosing $\eta(s)$ specifies the transformation. As in Ref. [12], we restrict ourselves to the simple choice [11]

$$\eta(s) = [T_{\mathrm{rel}}, H_s] \,, \tag{4}$$

which gives the flow equation,

$$\frac{dH_s}{ds} = [[T_{\rm rel}, H_s], H_s] = [[T_{\rm rel}, V_s], H_s] \,. \tag{5}$$

In a momentum basis, this choice suppresses off-diagonal matrix elements, forcing the hamiltonian towards a band-diagonal form.

The evolution in Eq. (5) includes all many-body components of the hamiltonian. In the space of relative momentum NN states only, it means that the partial-wave momentum-space potential evolves as (with normalization so that $1 = \frac{2}{\pi}\int_0^\infty q^2\, dq\, |q\rangle\langle q|$ and in units where $\hbar = c = m = 1$ with nucleon mass m),

$$\begin{aligned}\frac{dV_s(k,k')}{ds} =& -(k^2 - k'^2)^2\, V_s(k,k') \\ &+ \frac{2}{\pi}\int_0^\infty q^2\, dq\, (k^2 + k'^2 - 2q^2)\, V_s(k,q)\, V_s(q,k') \,. \end{aligned} \tag{6}$$

(The additional matrix structure of V_s in coupled channels such as ${}^3\mathrm{S}_1$–${}^3\mathrm{D}_1$ is implicit.) For matrix elements far from the diagonal, the first term on the right side of Eq. (6) dominates and exponentially suppresses these elements as s increases. By discretizing the relative momentum space on a grid of gaussian integration points, we obtain a simple (but nonlinear) system of first-order coupled differential equations, with the boundary condition that $V_s(k,k')$ at the initial $s = 0$ is equal to the initial potential. Since the SRG transformation is unitary, the NN phase shifts and deuteron binding energy calculated with H_s are independent of s to within numerical precision.

The evolution with s of any other operator O is given by the same unitary transformation, $O_s = U(s) O U^\dagger(s)$, which means that O_s evolves according to

$$\frac{dO_s}{ds} = [\eta(s), O_s] = [[T_{\rm rel}, V_s], O_s] \,. \tag{7}$$

Just as with the hamiltonian H_s, this evolution will induce many-body operators even if the initial operator is purely two-body. If we restrict ourselves to the relative momentum NN space, we have

$$\begin{aligned}\frac{dO_s(k,k')}{ds} =& \frac{2}{\pi}\int_0^\infty q^2\, dq \Big[(k^2 - q^2)\, V_s(k,q)\, O_s(q,k') \\ &+ (k'^2 - q^2)\, O_s(k,q)\, V_s(q,k') \Big] \,. \end{aligned} \tag{8}$$

To evolve a particular O_s simultaneously with V_s, we simply include the discretized version of Eq. (8) as additional coupled first-order differential equations.

An alternative, more direct, approach in the two-body space is to construct the unitary transformation at each s explicitly, and then use it to transform operators. Let $|\psi_\alpha(s)\rangle$ be an eigenstate of H_s with eigenvalue E_α (which is independent of s). Then $U(s)$ is given by

$$U(s) = \sum_\alpha |\psi_\alpha(s)\rangle\langle\psi_\alpha(0)| \,. \tag{9}$$

In a discretized partial-wave relative-momentum space with momenta $\{k_i\}$, we can solve for the eigenvectors of $H = H_{s=0}$ and H_s, then construct the matrix elements of $U(s)$ [which we denote $U_s(k_i, k_j)$] by summing over the product of momentum-space wave functions:

$$U_s(k_i, k_j) = \sum_\alpha \langle k_i|\psi_\alpha(s)\rangle\langle\psi_\alpha(0)|k_j\rangle \,. \tag{10}$$

In practice this is an efficient way to construct the unitary transformation and subsequently to evolve any operator in the two-body space.

3 Applying the SRG

In Ref. [12], the SRG was applied with chiral EFT interactions at N^{3}LO [14,15] as the initial potentials. It was shown that the simple SRG transformation drives the hamiltonian towards the diagonal (in momentum space), making it more perturbative and more convergent in few-body calculations. (In fact, it behaves just like a $V_{\mathrm{low}\,k}$ potential.) The parameter $\lambda \equiv s^{-1/4}$ provides a measure of the spread of off-diagonal strength in V_s. The V_s potential at λ was found to correspond roughly to a smoothly regulated $V_{\mathrm{low}\,k}$ interaction [16] with momentum cutoff $\Lambda \approx \lambda$. In this work, we also use the Argonne v_{18} [17] and the CD-Bonn [18] potentials as initial potentials in the SRG evolution. We find the same universal behavior [19].

In Fig. 1, phase shifts in selected partial waves up to laboratory energies of 1 GeV are shown for the Argonne v_{18} [17], CD-Bonn [18] and chiral N^{3}LO [14] potentials. [1] As expected for unitary transformations, the phase shifts at any λ are the same as those for the corresponding initial potential (up to numerical inaccuracies that are currently less than 0.1% in the worst case, with no real attempt at numerical optimization). The phase shifts from different initial potentials start to disagree for energies above 300–400 MeV. The fact that they lead to very similar low-momentum interactions [1,2,12] is an indication that all low-energy observables should similarly decouple after RG evolution.

[1] Nonrelativistic kinematics is used, which means that comparisons with experiment at higher energy should be made with caution. This can be improved but will not change our discussion because it will have no effect on low-energy observables.

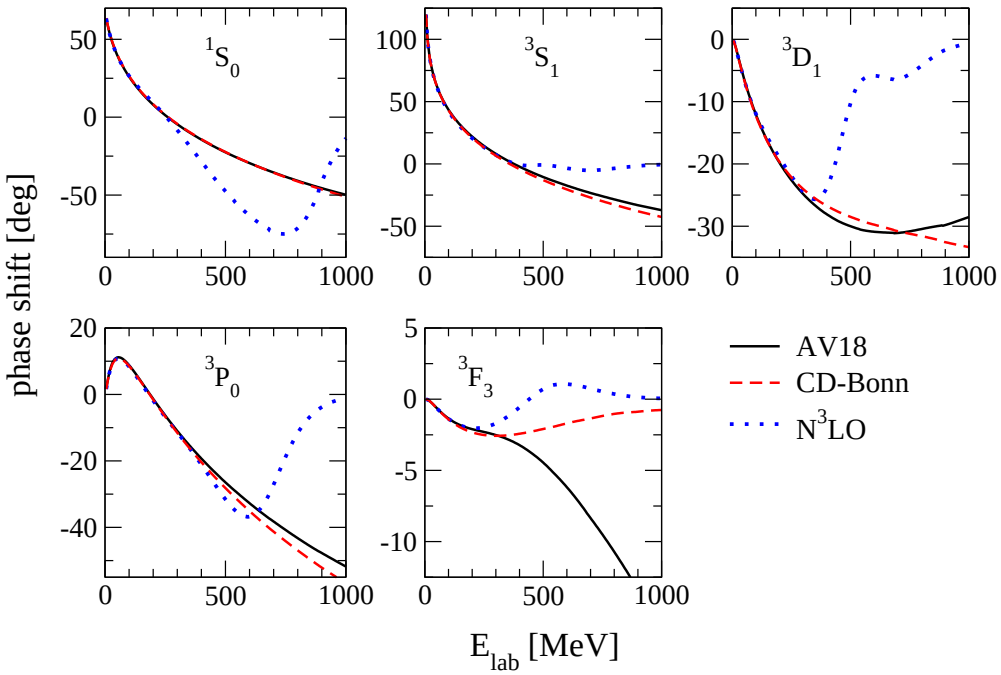

Fig. 1. Phase shifts for the Argonne v_{18} [17], CD-Bonn [18] and chiral N^{3}LO [14] potentials in selected channels (using nonrelativistic kinematics). The phase shifts after evolving in λ from each initial potential agree for all λ to within the widths of the lines at all energies.

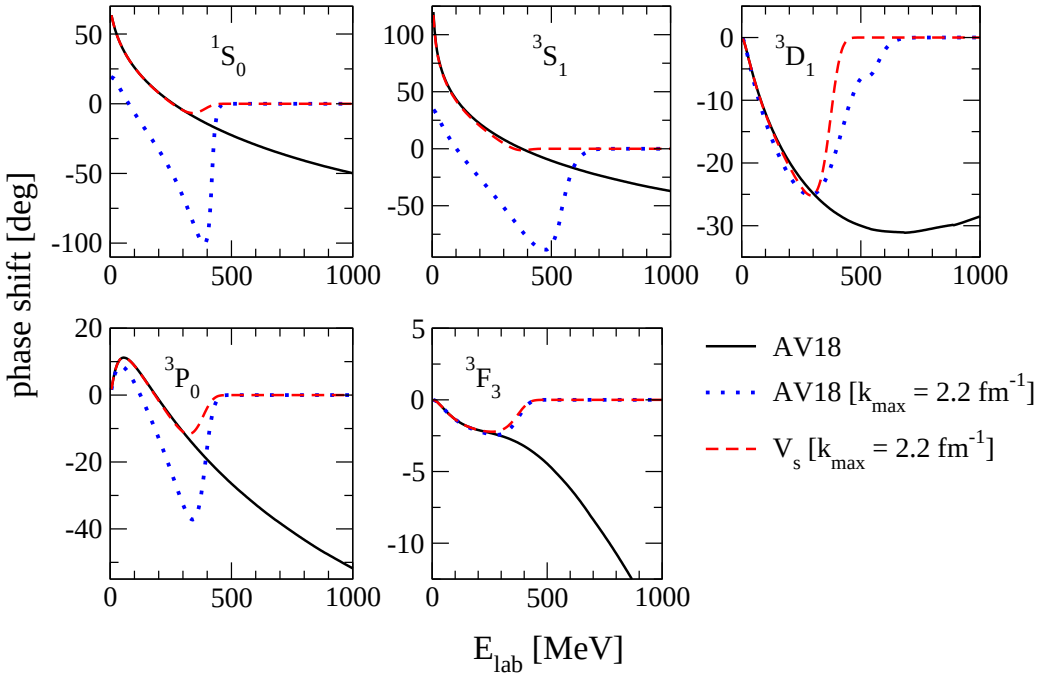

Fig. 2. Phase shifts in selected channels for the Argonne v_{18} potential [17] and when intermediate momenta $k > k_{\rm max} = 2.2\,{\rm fm}^{-1}$ are excluded. We contrast the latter results to the phase shifts obtained from the evolved V_s potential for $\lambda = 2\,{\rm fm}^{-1}$ and the additional constraint $k_{\rm max} = 2.2\,{\rm fm}^{-1}$.

But here we explicitly demonstrate this decoupling rather than relying on generic RG arguments.

We test the decoupling of high-energy details from low-energy phase shifts by setting $V_s(k,k')$ to zero for all k,k' above a specified momentum $k_{\rm max}$. Results for $k_{\rm max} = 2.2\,{\rm fm}^{-1}$ using a smooth regulator function are shown in Fig. 2 for the initial Argonne v_{18} potential and for the evolved V_s potential with $\lambda = 2.0\,{\rm fm}^{-1}$. The phase shifts for the initial potential in the lower partial waves bear no relation to the result without a $k_{\rm max}$ cutoff. [2] In contrast, the low-energy phase shifts for the SRG-evolved potential are unchanged, even though the high-energy phase shifts above $k_{\rm max}$ are now zero. The details of how the momentum is cut off affect only the behavior near $k_{\rm max}$. The deviation near $k_{\rm max}$ in Fig. 2 is consistent with the SRG (with the present choice of η) effectively imposing a rather smooth cutoff in momentum, similar to an exponential regulator with exponent $n_{\rm exp} = 2$, which is the analytic behavior for solutions of the linearized SRG equation. Finally, the angular momentum barrier in higher partial waves such as ${}^3{\rm F}_3$ ensures that cutting off high momentum has the same effect for all interactions since they share the same long-range one-pion exchange potential.

The deuteron binding energy provides another clear example of how the contributions of different momentum components to a low-energy observable depend on the resolution scale (as measured by λ or s). In Fig. 3, we show the kinetic, potential, and total energy from an integration in momentum space including momenta up to $k_{\rm max}$. That is, we plot

$$\begin{aligned} E_d(k<k_{\rm max}) &= T_{\rm rel}(k<k_{\rm max}) + V_s(k<k_{\rm max}) \\ &= \int_0^{k_{\rm max}} d\mathbf{k} \int_0^{k_{\rm max}} d\mathbf{k}'\, \psi_d^\dagger(\mathbf{k};\lambda) \left(k^2\delta^3(\mathbf{k}-\mathbf{k}') + V_s(\mathbf{k},\mathbf{k}') \right) \psi_d(\mathbf{k}';\lambda)\,, \end{aligned} \tag{11}$$

where $\psi_d(\mathbf{k};\lambda)$ is the momentum-space deuteron wave function from the corresponding potential V_s (without $k_{\rm max}$).

Figure 3 shows that the Argonne v_{18} potential [17] has large (and canceling) contributions from the high-momentum matrix elements of the hamiltonian. For example, if one excludes momenta greater than $2\,{\rm fm}^{-1}$ in the deuteron wave function when calculating the binding energy, the deuteron is 9.9 MeV unbound (that is, the integrated kinetic energy up to $2\,{\rm fm}^{-1}$ is 11.5 MeV while the potential energy is -1.6 MeV). One needs to include contributions up to $4\,{\rm fm}^{-1}$ to even get a bound state. In contrast, using V_s with $\lambda = 2\,{\rm fm}^{-1}$, we see that the converged result is dominated by contributions from much lower

[2] The coupling between high and low momentum for the Argonne potential is so strong in the coupled ${}^3{\rm S}_1$–${}^3{\rm D}_1$ channel that we had to use a slightly larger $k_{\rm max} = 2.5\,{\rm fm}^{-1}$ with a smoother regulator just to keep the phase shifts on the plot.

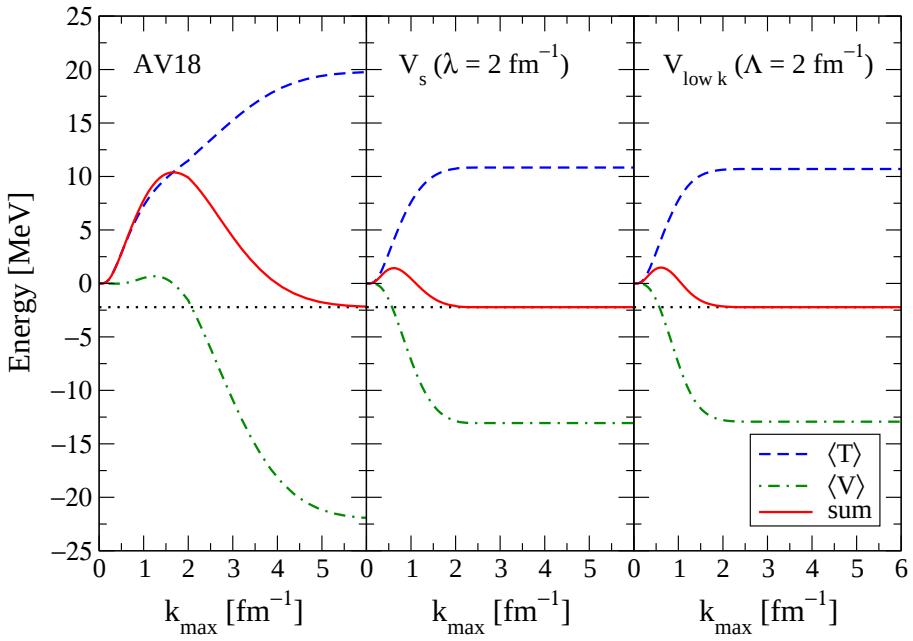

Fig. 3. Expectation values in the deuteron of the kinetic, potential, and total energy evaluated in momentum space as a function of the maximum momentum $k_{\max}$, see Eq. (11). Results are shown for the Argonne v_{18} potential [17] (left), the evolved V_s potential for $\lambda = 2\,\mathrm{fm}^{-1}$, and the smooth-cutoff $V_{\mathrm{low}\,k}$ interaction with $\Lambda = 2\,\mathrm{fm}^{-1}$ and exponential regulator $n_{\exp} = 2$

momenta.[3] Note that the V_s potential has no appreciable contributions above λ, even though the near-diagonal matrix elements of the potential $V_s(k,k')$ for $k, k' > k_{\max}$ are not negligible. This again validates the advertised decoupling. We also see that the V_s and $V_{\mathrm{low}\,k}$ results are very similar for $\lambda \approx \Lambda$, where Λ is the momentum cutoff for $V_{\mathrm{low}\,k}$.

We turn to the momentum distribution in the deuteron next. The momentum distribution at relative momentum $\mathbf{q}$ is the expectation value of $a^\dagger_{\mathbf{q}} a_{\mathbf{q}}$ (summed over spin substates M_S) and is proportional to the sum of the squares of the normalized S-wave and D-wave parts of the deuteron wave function, $u(q)^2 + w(q)^2$. It is not directly related to an observable [20]. As discussed in Sect. 2, using the SRG we can consistently evolve operators in s (or λ). In particular, we can evolve $a^\dagger_{\mathbf{q}} a_{\mathbf{q}}$ starting from a given hamiltonian. Since the SRG proceeds via unitary transformations, no information is lost, by construction. But even more, we can show explicitly that by evolving to a low-momentum interaction, we decouple the low-momentum and high-momentum physics in a low-energy state.

[3] We can also simply set the high-momentum matrix elements of V_s to zero (that is, exclude momenta larger than $k_{\max}$ at the level of the hamiltonian), and then solve for the deuteron. For $\lambda = 2\,\mathrm{fm}^{-1}$, choosing $k_{\max} = 2.2\,\mathrm{fm}^{-1}$ only changes the binding energy to 2.2 MeV, while raising $k_{\max}$ slightly yields the full V_s result.

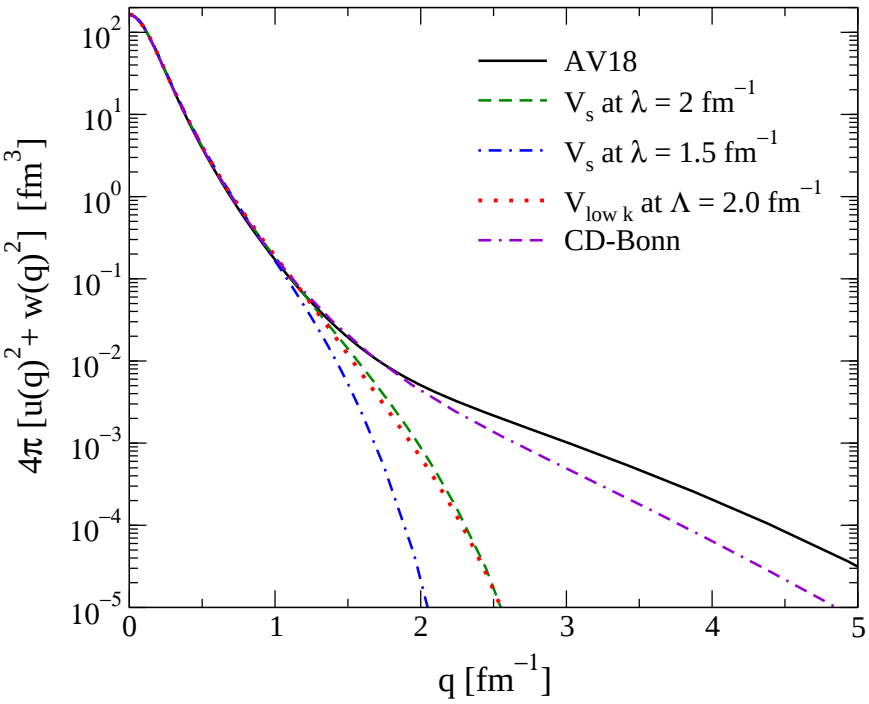

Fig. 4. Deuteron momentum distribution $\langle a^\dagger_{\mathbf{q}} a_{\mathbf{q}} \rangle_d \propto u(q)^2 + w(q)^2$ using the Argonne v_{18} [17], CD-Bonn [18] and SRG potentials evolved from Argonne v_{18} to $\lambda = 1.5\,\mathrm{fm}^{-1}$ and $2\,\mathrm{fm}^{-1}$ (but not evolving the operator), and a smooth-cutoff $V_{\mathrm{low}\,k}$ interaction with $\Lambda = 2\,\mathrm{fm}^{-1}$ and exponential regulator $n_{\mathrm{exp}} = 2$.

In Fig. 4, we plot deuteron matrix elements of $a^\dagger_{\mathbf{q}} a_{\mathbf{q}}$ for the Argonne v_{18} [17] and CD-Bonn [18] potentials, as well as for two SRG and a smooth-cutoff $V_{\mathrm{low}\,k}$ interaction evolved from Argonne v_{18}. We emphasize again that matrix elements of this operator are not measurable, so one should not ask which of these is the "correct" momentum distribution in the deuteron; it is a potential- and scale-dependent quantity. It is evident that the V_s distributions have substantial momentum components only for k below λ, and that the $V_{\mathrm{low}\,k}$ distribution is very similar to the corresponding V_s distribution. Nevertheless, if we use the SRG- or RG-evolved operator with these deuteron wave functions, we precisely reproduce the momentum distribution from the original potential at *all momenta* and for *all* λ.

This result by itself is guaranteed by construction. The more interesting issue is where the strength of the matrix element comes from. For example, for the bare operator and the Argonne v_{18} potential, the momentum distribution at $q = 4\,\mathrm{fm}^{-1}$ comes entirely from deuteron wave function components at that momentum. But when $\lambda = 2\,\mathrm{fm}^{-1}$, it is clear from Fig. 4 that the deuteron does not have appreciable momentum components above $2.5\,\mathrm{fm}^{-1}$ (even though V_s does near the diagonal [12]). In Fig. 5, we take the ratio of the evolved operator evaluated with the evolved wave function at q to the corresponding initial quantity, but include in the numerator only momenta up to k_{max}. The

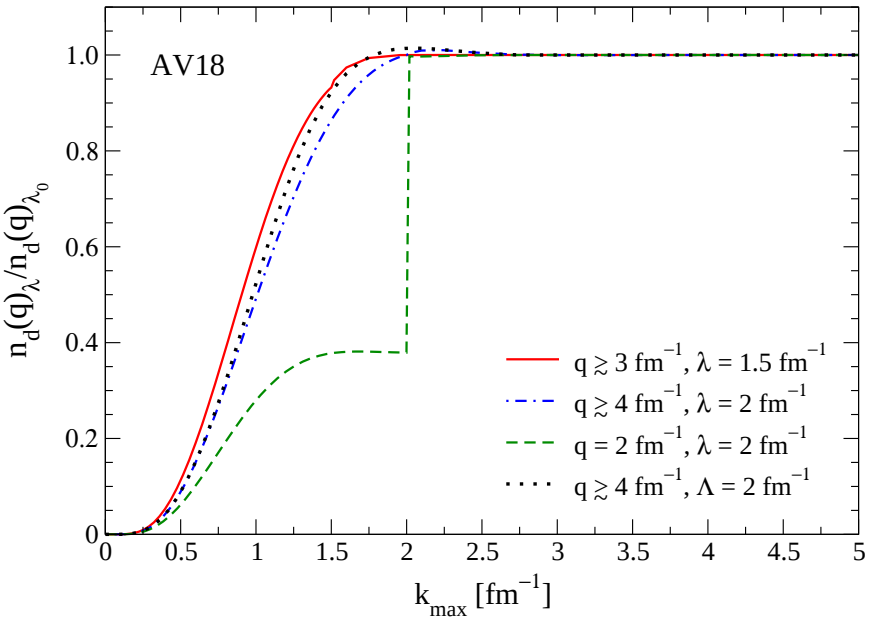

Fig. 5. Ratio of the deuteron momentum distribution at various momenta q evolved from the Argonne v_{18} potential [17] via the SRG to the corresponding initial momentum distribution, as a function of the maximum momentum $k_{\rm max}$ in the deuteron wave functions in the numerator. Note that the un-evolved Argonne v_{18} result is simply a step function at q. For comparison, we also show the result for a smooth–cutoff $V_{{\rm low}\,k}$ interaction with $\Lambda = 2\,{\rm fm}^{-1}$ and exponential regulator $n_{\rm exp} = 2$.

numerator is thus:

$$\int_0^{k_{\rm max}} d\mathbf{k} \int_0^{k_{\rm max}} d\mathbf{k}'\, \psi_d^\dagger(\mathbf{k};\lambda) U_\lambda(\mathbf{k},\mathbf{q}) U_\lambda^\dagger(\mathbf{q},\mathbf{k}') \psi_d(\mathbf{k}';\lambda)\,. \tag{12}$$

We observe that for all q, the ratio approaches unity for large enough $k_{\rm max}$, as dictated by the unitary transformation. For $\lambda = 1.5\,{\rm fm}^{-1}$ or $2\,{\rm fm}^{-1}$, larger values of q ($q \gtrsim 3\,{\rm fm}^{-1}$ or $q \gtrsim 4\,{\rm fm}^{-1}$, respectively) give results approximately independent of q, with a smooth approach to unity by $k_{\rm max} \approx 1.3\lambda$. This is consistent with the operator $U_\lambda(\mathbf{k},\mathbf{q})$ factorizing into $K_\lambda(\mathbf{k})\, Q_\lambda(\mathbf{q})$ for $k < \lambda$ and $q \gg \lambda$, and thus the q dependence cancels in the ratio. It remains to be seen whether this factorization is a general feature that can be understood using operator product expansion ideas [13]. For small q, the original step function is essentially preserved (not shown). For q of order λ, there is a step behavior at λ but some strength is shifted to lower k, k'. In all cases the flow of the operator strength weighted by ψ_d is toward lower momenta. The ratio for the smooth-cutoff $V_{{\rm low}\,k}$ is very similar at low $k_{\rm max}$ and for $k_{\rm max}$ approaching Λ/λ. Finally, we have verified that taking matrix elements using even a rough variational ansatz for the wave function also works fine, which serves as a check that there is no fine-tuning in the evolved operator.

4 Conclusions

Renormalization theory tells us that low-energy physics does not depend on the details of the high-energy dynamics. The high-energy information we *do* need can be incorporated in nuclear interactions using renormalization group methods designed to handle similar problems in relativistic field theories and critical phenomena in condensed matter systems. This means that we can decouple the physics of low energy from high energy, drastically reducing the number of explicit degrees of freedom required for precise non-perturbative low-energy calculations.

But while it is possible to decouple low- and high-energy physics, it does not happen automatically. We have seen that when using conventional NN potentials with strong short-range repulsion, such as Argonne v_{18} [17], there are momentum contributions that are high on nuclear scales but must be included, or else even very low-energy observables will be incorrect. We emphasize that the need for high-momentum components in these particular calculations *does not* imply that the high-energy description is correct (or measurable).

Two-nucleon interactions derived via the SRG explicitly decouple low-energy physics from detailed high-momentum dynamics. Using SRG potentials we have shown that high-energy details in wave functions and operators are irrelevant to low-energy observables. *When we set the high-momentum components to zero in V_s potentials with low λ, there is no noticeable loss of information:* The low-energy phase shifts and expectation values in the deuteron are practically unchanged. A corollary is that statements about high-momentum parts in the deuteron or any other bound state depend on the potential or scale. This also holds for expectation values of other operators, such as the one-pion exchange potential or three-nucleon interactions. Finally, our results imply that there is also no problem with effective field theory interactions that predict zero phase shifts above a cutoff.

Using the SRG, operators can be evolved, including those associated with high momenta in initial potentials, so that matrix elements in low-energy states (like the deuteron) are unchanged. We find for the momentum distribution that the operator strength flows toward lower momentum, so the matrix elements do not change even after contributions from high momenta are excluded. We also observe that the ratio of evolved to initial deuteron momentum distribution is nearly independent of momentum q at fixed λ for sufficiently large q, which motivates an investigation using an operator product expansion.

In the past, unitary transformations of NN potentials were applied to calculations of few-body systems and nuclear matter. Results for observables depended on the transformations and this was often the context for discussing

"off-shell" effects and which was the "true potential". From the modern perspective, this approach is misleading at best. These transformations always lead to many-body interactions, even if absent in the initial hamiltonian. While this fact was clearly recognized in past investigations [21], many-body forces were usually neglected. The SRG is one promising approach to evolve consistent three-nucleon interactions. Once the three-body SRG is implemented, the tests of decoupling can be extended to systems with more than two nucleons.

Acknowledgements

This work was supported in part by the National Science Foundation under Grant No. PHY–0354916 and the Natural Sciences and Engineering Research Council of Canada (NSERC). TRIUMF receives federal funding via a contribution agreement through the National Research Council of Canada.

References

[1] S.K. Bogner, T.T.S. Kuo, A. Schwenk, D.R. Entem and R. Machleidt, Phys. Lett. B **576** (2003) 265.

[2] S.K. Bogner, T.T.S. Kuo and A. Schwenk, Phys. Rept. **386** (2003) 1.

[3] S.K. Bogner, A. Schwenk, T.T.S. Kuo and G.E. Brown, nucl-th/0111042.

[4] A. Nogga, S.K. Bogner and A. Schwenk, Phys. Rev. C **70** (2004) 061002(R).

[5] S.K. Bogner, A. Schwenk, R.J. Furnstahl and A. Nogga, Nucl. Phys. **A763** (2005) 59.

[6] S.K. Bogner, T.T.S. Kuo, L. Coraggio, A. Covello and N. Itaco, Phys. Rev. C **65** (2002) 051301(R).

[7] A. Schwenk and A.P. Zuker, Phys. Rev. C **74** (2006) 061302(R).

[8] O. Benhar and V.R. Pandharipande, Phys. Rev. C **47** (1993) 2218.

[9] S.D. Glazek and K.G. Wilson, Phys. Rev. D **48** (1993) 5863; Phys. Rev. D **49** (1994) 4214.

[10] F. Wegner, Ann. Phys. (Leipzig) **3** (1994) 77.

[11] S. Szpigel and R.J. Perry, in Quantum Field Theory, A 20th Century Profile, Ed. A.N. Mitra, Hindustan Publishing Com., New Delhi, 2000, hep-ph/0009071.

[12] S.K. Bogner, R.J. Furnstahl, and R.J. Perry, nucl-th/0611045.

[13] G.P. Lepage, "How to Renormalize the Schrödinger Equation", Lectures given at 9th Jorge Andre Swieca Summer School: Particles and Fields, Sao Paulo, Brazil, February, 1997, nucl-th/9706029.

[14] D.R. Entem and R. Machleidt, Phys. Rev. C **68** (2003) 041001(R).

[15] E. Epelbaum, W. Glöckle and U.G. Meißner, Nucl. Phys. **A747** (2005) 362.

[16] S.K. Bogner, R.J. Furnstahl, S. Ramanan and A. Schwenk, Nucl. Phys. **A** in press, nucl-th/0609003.

[17] R.B. Wiringa, V.G.J. Stoks and R. Schiavilla, Phys. Rev. C **51** (1995) 38.

[18] R. Machleidt, Phys. Rev. C **63** (2001) 024001.

[19] See http://www.physics.ohio-state.edu/∼ntg/srg/ for documentary examples.

[20] R. J. Furnstahl and H. W. Hammer, Phys. Lett. B **531** (2002) 203.

[21] F. Coester, S. Cohen, B. Day, and C.M. Vincent, Phys. Rev. C **1** (1970) 769.